Acta Crystallographica Section B
Structural Science
ISSN 0108-7681

Structures of alkyl-substituted Tröger's base derivatives illustrate the importance of Z' for packing in the absence of strong crystal synthons

Christophe M. L. Vande Velde,[a,b]* Benoît Tylleman,[b] Matthias Zeller[c] and Sergey Sergeyev[b,d]

[a]Karel de Grote University College, Department of Applied Engineering, Salesianenlaan 30, 2660 Antwerp, Belgium, [b]Université Libre de Bruxelles (ULB), Laboratoire de Chimie des Polymères, CP 206/01, Boulevard du Triomphe, 1050 Brussels, Belgium, [c]Youngstown State University, Department of Chemistry, One University Plaza, Youngstown, OH 44555-3663, USA, and [d]University of Antwerp, Department of Chemistry, Groenenborgerlaan 171, 2020 Antwerp, Belgium

Correspondence e-mail: christophe.vandevelde@kdg.be

Received 14 February 2010
Accepted 8 June 2010

Crystal structures of Tröger's base (5,11-methano-2,8-dimethyl-5,6,11,12-tetrahydrodibenzo[*b*,*f*][1,5]diazocine) analogues with the methyl groups replaced by ethyl, *iso*-propyl and *tert*-butyl groups were studied. The incidence of $Z' > 1$ structures increases to rather conspicuous levels. The reasons behind this trend are expanded upon, and a possible explanation is given in the flexibility of the alkyl substituents and van der Waals stabilization. In combination these effects allow for an additional stabilization of the packing by small changes in the molecular conformations, thus expanding the size of the asymmetric unit.

1. Introduction

At the time of writing, the reasons for the phenomenon of crystallization with $Z' > 1$, or, in other words, several molecules within one unit cell which are unrelated by crystallographic symmetry and in some cases also have different geometries – are not well understood. The statement has been made that high Z' structures are often a commensurate modulation of a simpler parent structure with $Z' = 1$, which would allow minimization of mismatch spacing between molecules (Hao *et al.*, 2005). Competing strong directional interactions, or directional interactions in combination with chirality of the molecule, have been pointed out as particularly common in crystal structures with $Z' > 1$ (Anderson *et al.*, 2008; Anderson & Steed, 2007; Desiraju, 2007; Steed, 2003), and at an earlier occasion, stress has been placed on molecular shape as a driving factor (Pidcock, 2006). Others have been more careful in stating that 'at present one cannot go beyond the conclusion that $Z' > 1$ is just one of the many options that organic molecules can take during the highly complex and still to a large extent mysterious process of coalescence and crystallization' (Gavezzotti, 2008).

In this paper we will investigate the crystal structures of a series of substituted Tröger's base analogues which are chiral,

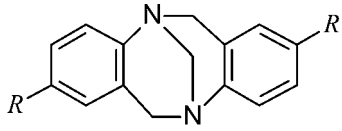

(1)-(4) (1) R = Me
(2) R = Et
(3) R = i-Pr
(4) R = t-Bu

Figure 1
Structural formulae of compounds (1)–(4). The following nomenclature is adopted for the crystal structures: indices *a* refer to the racemic, and *b* to the enantiomerically pure compounds. Thus, (1*a*) and (1*b*) are structures of the racemic and enantiomerically pure Tröger's base, respectively.

but lack strong, directional intermolecular interactions. Tröger's base, (±)-5,11-methano-2,8-dimethyl-5,6,11,12-tetrahydrodibenzo[*b*,*f*][1,5]diazocine [(1), Fig. 1], a chiral diamine with two stereogenic bridgehead N atoms, was first synthesized in 1887 by the condensation of *para*-methylaniline with formaldehyde (Tröger, 1887).

A unique set of structural features (chirality in combination with a relatively rigid V-shape geometry and a distance of *ca* 10 Å between the extremities of the scaffold) makes derivatives of Tröger's base very attractive for applications in supramolecular chemistry and molecular recognition (for recent reviews on history, synthetic chemistry and applications of Tröger's base, see Sergeyev, 2009; Dolenský *et al.*, 2007, and references therein). If we consider the set of 6*H*,12*H*-5,11-methanodibenzo[*b*,*f*][1,5]diazocine derivatives, excluding salts, solvates, co-crystals and substances with the benzene rings as a part of a larger (hetero)aromatic system, or with substituents elsewhere than on the benzene rings, a total of 37 structures has been published to date [CSD Version 5.31; Allen, 2002; with three updates up to May 2010]. In all structures, the overall V shape of the molecule persists, while the angle between the two aromatic rings can vary between *ca* 85 and 110° (Dolenský *et al.*, 2007). We have chosen a series of Tröger's base analogues for the investigation of the structure and packing in the absence of strong interactions due to hydrogen bonding or strongly polar functional groups. To this end, the methyl groups of Tröger's base were substituted by progressively larger alkyl groups. Altogether six structures of racemic and enantiopure Tröger's base analogues (2)–(4) with ethyl, *iso*-propyl and *tert*-butyl substituents were determined. Displacement ellipsoid plots with numbering schemes of structures (2*a*), α-(3*a*), β-(3*a*), γ-(3*a*), (4*a*) and (4*b*) are provided in Fig. 2.

We will demonstrate that the members of this particular series of chiral molecules, which do not have strongly directional crystal synthons, nevertheless have a preference for crystallization with $Z' > 1$. Since no strong directional interactions are able to stabilize the structures, the shape of the van der Waals envelope of the molecules should be the determining factor in the formation of long-range order. We will conclude by observing which of the existing theories on $Z' > 1$ fits these observations best.

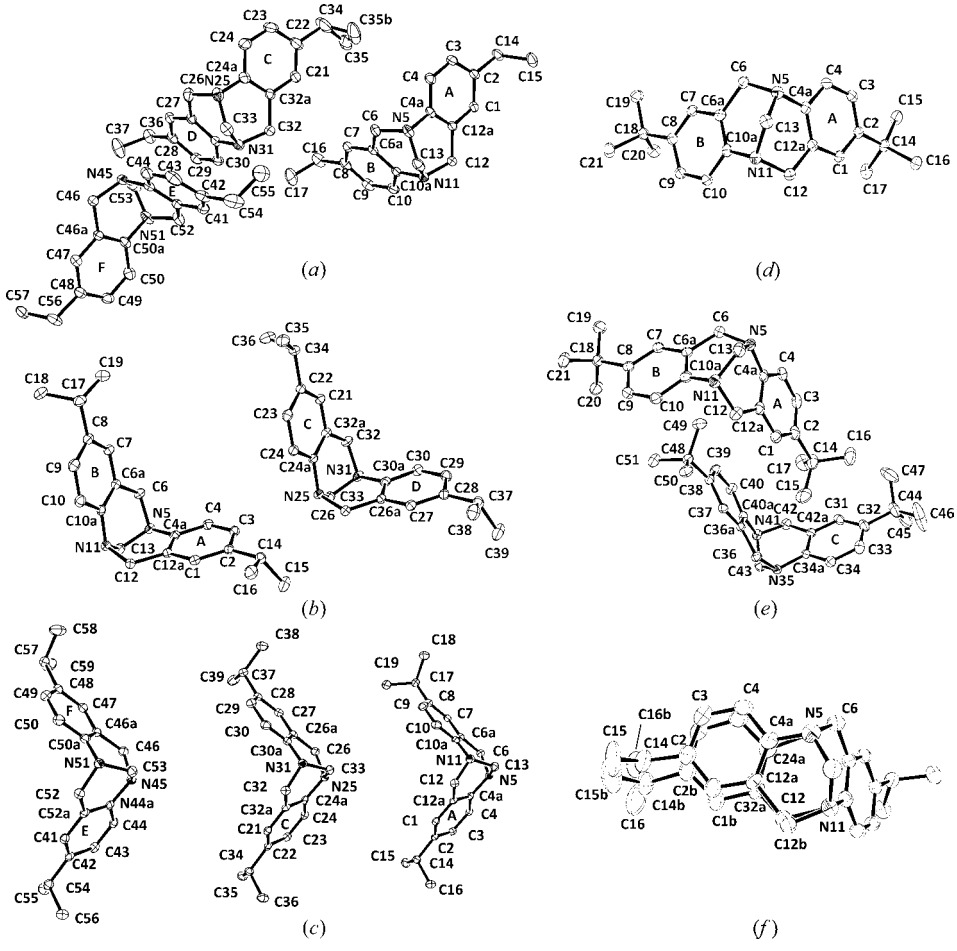

Figure 2
Displacement ellipsoid plots at the 50% probability level of (*a*) (2*a*), (*b*) α-(3*a*), (*c*) β-(3*a*), (*d*) γ-(3*a*), (*e*) (4*a*) and (*f*) (4*b*). H atoms are omitted for clarity. Rings are denominated by capital letters. Not all atoms or rings are annotated for reasons of clarity, but missing letters and numbers are easily inferred since the numbering between molecules is consistent.

2. Experimental

Compounds (2)–(4) were synthesized as racemates from the corresponding anilines, according to a previously published procedure. The resolution of (2)–(4) was achieved by preparative chromatography on the commercially available chiral stationary phase Whelk O1 (Regis Technologies Inc., USA). For experimental details and analytical data, we refer the reader to Didier *et al.* (2008).

Crystals suitable for single-crystal X-ray diffraction experiments were grown by slow evaporation of dichloromethane solutions in all cases, except (2*a*) which was crystallized by slow evaporation of an ethanolic solution. Data sets were collected on a Bruker three-circle goniometer with Smart APEX [(2*a*), α-(3*a*), β-(3*a*), γ-(3*a*), (4*b*)] or APEXII [(4*a*)] detector, employing graphite-monochromated Mo *Kα* radiation. Crystals were flash-cooled in a nitrogen atmosphere to 90 or 100 K by means of a cold nitrogen gas stream (Cryostream/Kryoflex), except for γ-(3*a*), which was collected at 148 K. For further details on β-(3*a*) and γ-(3*a*) see §3.

Table 1
Crystallographic data for structures (2)–(4).

	(2*a*)	α-(3*a*)	β-(3*a*)	γ-(3*a*)	(4*a*)	(4*b*)
Crystal data						
Chemical formula	$C_{19}H_{22}N_2$	$C_{21}H_{26}N_2$	$C_{21}H_{26}N_2$	$C_{21}H_{26}N_2$	$C_{23}H_{30}N_2$	$C_{23}H_{30}N_2$
M_r	278.40	306.44	306.44	306.44	334.49	334.49
Crystal system, space group	$P\bar{1}$	$P\bar{1}$	$P2_1/c$	$P2_1/c$	$P2_1/c$	$C2$
Temperature (K)	100	100	100	148	90	100
a, b, c (Å)	10.9907 (11), 13.8123 (14), 17.2240 (17)	7.6347 (11), 15.454 (2), 15.936 (2)	14.944 (2), 33.259 (4), 10.754 (1)	14.985 (3), 11.195 (2), 10.746 (2)	15.529 (4), 12.186 (3), 10.764 (2)	28.370 (2), 6.6841 (5), 21.6271 (16)
α, β, γ (°)	71.4690 (10), 88.621 (2), 70.3190 (10)	66.214, 82.257 (2), 85.370 (2)	90, 104.713 (2), 90	90, 104.873 (2), 90	90, 110.147 (6), 90	90, 105.940 (1), 90
V (Å^3)	2324.2 (4)	1704.1 (4)	5169.4 (10)	1742.3 (3)	1912.3 (8)	3943.4 (5)
Z	6	4	12	4	4	8
μ (mm^{-1})	0.07	0.07	0.07	0.07	0.07	0.07
Crystal size (mm^3)	0.46 × 0.43 × 0.36	0.45 × 0.45 × 0.41	0.48 × 0.18 × 0.10	0.69 × 0.22 × 0.10	0.25 × 0.2 × 0.15	0.45 × 0.25 × 0.21
Data collection						
Diffractometer	Bruker Smart APEX	Bruker Smart APEX	Bruker Smart APEX	Bruker Smart APEX	Bruker APEXII	Bruker Smart APEX
Absorption correction	Bruker *SADABS*-2008/1	Bruker *SADABS*-2008/1	Bruker *SADABS*-2008/1	Bruker *SADABS*-2008/1	Bruker *SADABS*-2007/4	Bruker *SADABS*-2008/1
T_{min}, T_{max}	0.899, 0.978	0.794, 0.970	0.680, 0.746	0.623, 0.746	0.858, 0.989	0.648, 0.746
No. of measured, independent and observed [$I > 2\sigma(I)$] reflections	27 074, 13 682, 10 156	19 493, 10 060, 6632	47 709, 12 803, 9089	17 929, 5112, 2968	31 760, 3955, 3197	17 606, 6393, 4971
R_{int}	0.021	0.035	0.049	0.038	0.046	0.050
Refinement						
$R[F^2 > 2\sigma(F^2)]$, $wR(F^2)$, S	0.055, 0.156, 1.02	0.053, 0.159, 0.99	0.068, 0.143, 1.11	0.047, 0.135, 1.03	0.046, 0.121, 1.14	0.054, 0.120, 1.01
No. of reflections	13 682	10 060	12 803	5112	3955	6393
No. of parameters	626	453	679	275	247	488
Restraints	8	0	0	10	0	1
H-atom treatment	Riding	Riding	Mixture of independent and constrained	Mixture of independent and constrained	Mixture of independent and constrained	Riding
$\Delta\rho_{max}$, $\Delta\rho_{min}$ (e Å^{-3})	0.46, −0.30	0.54, −0.28	0.32, −0.25	0.21, −0.18	0.27, −0.23	0.31, −0.25

Absolute structure of (4*b*) not determined, Friedel equivalents merged. Computer programs used: Bruker *SAINT* (Bruker, 2008), *SHELXS*86, *SHELXS*97, *SHELXL*97 (Sheldrick, 2008), *ORTEP*3 for Windows (Farrugia, 1997), *Mercury* (Bruno *et al.*, 2002), *WinGX* (Farrugia, 1999), *PLATON* (Spek, 2009).

Data were collected with ω scans. H atoms were placed in calculated positions after observation in a difference-Fourier map and their distances were refined [except the disordered parts in γ-(3*a*)]. For (4*b*) Friedel equivalents were merged. For all other details of the structure refinement and the software used, see Table 1.

Calculations with the UNI force field (Filippini & Gavezzotti, 1993; Gavezzotti & Filippini, 1994) were performed with the *OPIX* software (Gavezzotti, 2003), starting from the experimental geometries with idealized hydrogen positions.

3. Results and discussion

We start the discussion with the previously published structure of enantiopure Tröger's base (1*b*), which crystallizes in the space group $P2_12_12_1$ with one molecule in the asymmetric unit. The melting point is 400–401 K (Prelog & Wieland, 1944). The crystal structure was determined (at 293 K) by Worlitschek *et al.* (2004; CSD refcode AXAGEL). The molecules are stacked in slanted columns with a CH$\cdots\pi$ interaction between a non-bridging CH_2 and a ring carbon within the columns. Between the columns, the molecules display edge-to-face CH$\cdots\pi$ contacts above the van der Waals radius on one side, and below the van der Waals radius on the other side. In the *b* direction the columns are connected by an interaction between a methyl H and N.

Racemic Tröger's base (1*a*), also a previously reported structure (Larson & Wilcox, 1986; CSD refcode DILLEP), adopts a packing with two crystallographically independent molecules in the unit cell (and $Z' = 1, 5$), in the space group *Pccn*. (*S*,*S*) and (*R*,*R*) enantiomers alternate between columns positioned side-by-side. This leads to CH$\cdots\pi$ contacts of the bridging methylene group to each of the two benzene rings of the molecule on top. Between the columns there are areas where methyl groups from four columns are brought together to within their van der Waals distances, while the remaining four methyl groups are within the van der Waals distances of skeleton methylene groups. The melting point of this arrangement is higher than that of the enantiopure modification (409–410 K; Prelog & Wieland, 1944), implying that the

overall fit and packing stabilization energy is higher for the racemic crystal which elegantly explains why spontaneous resolution does not occur.

The racemic Tröger's base analogue with ethyl instead of methyl groups (2*a*) also does not resolve spontaneously, and moreover, the chromatographically separated enantiomers (Didier *et al.*, 2008) did not crystallize in our hands. Racemic crystals, however, could be obtained in the space group $P\bar{1}$, with D_x (100 K) = 1.193 g cm^{-3} and melting point 325–326 K.

The asymmetric unit of (2*a*), at 100 K, features three independent molecules, of which one has a single disordered ethyl group. Angles between the benzene ring planes of the Tröger's bases are 103.04 (7), 100.10 (6) and 99.76 (7)°. The packing motif of (2*a*) departs radically from that of Tröger's base itself, not forming stacks at all but instead forming pairs of enantiomers, in which the ethyl group of one molecule fills the cavity of the other. The tripling of the asymmetric unit with respect to the 'expected' structure with all molecular pairs equal and having inversion symmetry results from slight packing mismatches between the pairs of enantiomers, destroying the centre of symmetry within two of them. The first molecule, C1–C17, indicated in yellow in Fig. 3, packs in layers in the *ab* plane (we will call these 'layer 1') pairing up with its own symmetry equivalent. The two other molecules (red and blue in Fig. 3) form a (very similar) pair between them, in two layers (we will call these 'layer 2') before one layer of molecule 1 is repeated.

In the *c* direction, the order of the layers is thus 1–2–2–1–2–2– *etc*. Pseudo-translation symmetry can clearly be observed along the cell diagonal in the direction [$\bar{1}\bar{1}1$]. In Fig. 3 it can be easily seen that from the bottom-left corner of the cell a very similar pattern of pairs of molecules repeats three times to the top-right of the cell. A superimposed view of the three molecules by looking in the direction of the pseudo-translation is shown in Fig. 4.

The displacement of equivalent atoms within the three molecules after pseudo-translation (−0.333*a*, −0.333*b*, +0.333*c*) is quite significant and is on average (non-H atoms) 0.38 (1–2), 0.36 (2–3) and 0.62 Å (1–3) for the three molecules. The structure can thus also be seen as a commensurately modulated structure based on a parent structure with a third of the volume and $Z' = 1$. Unfortunately, we could not verify whether the structure transforms to the averaged structure at higher temperatures. The original data collection was performed with a flash-cooled crystal at 100 K, and the sample had not been retained. Repeated attempts to regrow single crystals of (2*a*) have been unsuccessful so far. The data from β-(3*a*) and γ-(3*a*) (high- and low-temperature polymorphs of the same compound, see below) however suggest that a high-temperature modification with $Z' = 1$ is quite possible. Another concern is the flash-cooling of the crystal, which could give rise to the freezing-in of a lattice vibration, in this way leading to modulation. For the same reasons as outlined above, we have been unable to confirm or refute this possibility due to our inability to re-crystallize (2*a*), but again, the data from β-(3*a*) and γ-(3*a*) show that the transition there is reversible, and does not correspond to a kinetic phenomenon, but to a real (local) potential minimum.

Despite the quite large modulation in (2*a*) it can be transformed to a subcell of one third the size, and can be success-

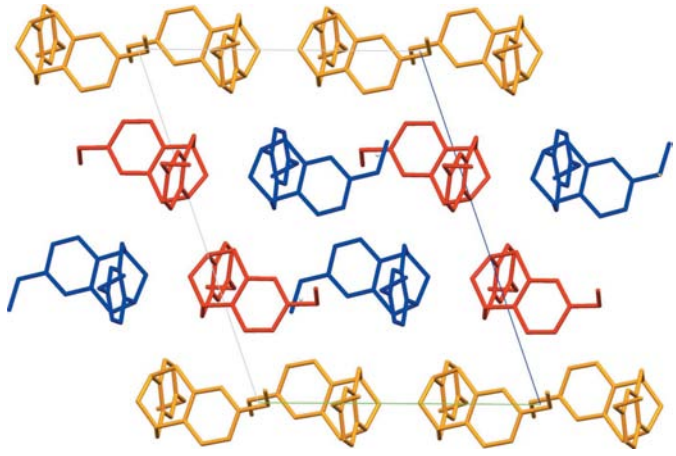

Figure 3
The packing of (2*a*), viewed along the *a* axis. Symmetry-equivalent molecules are identically colored. For further explanation, see text.

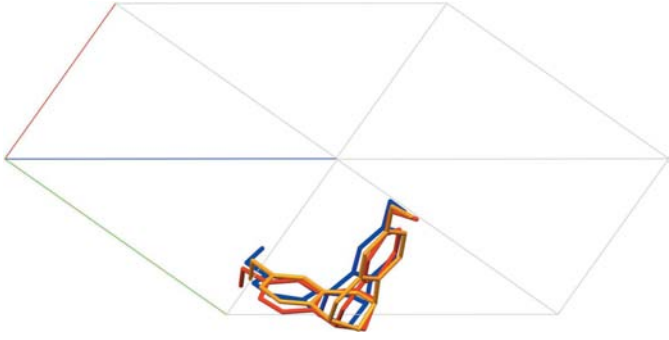

Figure 4
Superimposed view of the three symmetry-independent molecules in the structure of (2*a*) displaying pseudo-translation symmetry in the [$\bar{1}\bar{1}1$] direction.

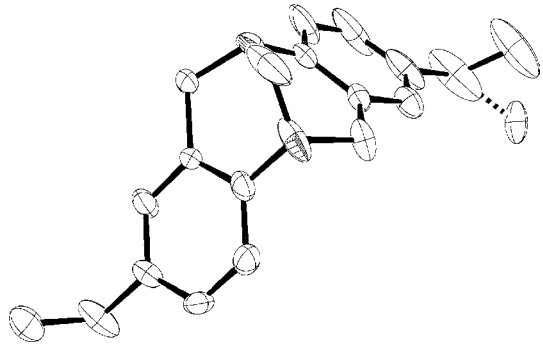

Figure 5
Displacement ellipsoid plot of the averaged structure (2*a*sub), at the 50% probability level. H atoms omitted for clarity. Minor disorder components of the ethyl group are indicated by the dashed bond.

Table 2
Crystallographic data for (sub)structures (2*a*), α-(3*a*) and β-(3*a*).

	(2*a*)	(2*a*sub)	α-(3*a*)	α-(3*a*sub)	β-(3*a*)	β-(3*a*sub)
Crystal data						
V (Å^3)	2324.2 (4)	774.7 (1)	1704.1 (4)	852.07 (4)	5169 (1)	1722.9 (7)
Crystal system, space group	Triclinic, $P\bar{1}$	Triclinic, $P\bar{1}$	Triclinic, $P\bar{1}$	Triclinic, $P\bar{1}$	Monoclinic, $P2_1/c$	$P2_1/c$
a, b, c (Å)	10.9907 (11), 13.8123 (14), 17.2240 (17)	7.8192 (5), 8.3866 (9), 11.8750 (13)	7.6347 (11), 15.454 (2), 15.936 (2)	7.6347 (11), 8.5751 (9), 13.1477 (13)	14.944 (2), 33.258 (4), 10.754 (1)	14.944 (2), 11.086 (4), 10.754 (1)
α, β, γ (°)	71.4690 (10), 88.621 (2), 70.3190 (10)	89.417 (4), 86.488 (6), 85.329 (19)	66.214, 82.257 (2), 85.370 (2)	88.077 (13), 82.583 (2), 86.993 (3)	90, 104.713 (2), 90	90, 104.713 (2), 90
Z	6	2	4	2	12	4
Z'	3	1	2	1	3	1
Data collection						
No. of measured, independent and observed [$I > 2\sigma(I)$] reflections	27 074, 13 682, 10 156	9009, 4554, 3655	19 493, 10 060, 6632	9669, 5029, 3899	47 709, 12 803, 9089	17 385, 5062, 3703
Reflection % with $I > 2\sigma(I)$	74.22	81.24	65.63	77.53	70.99	73.15
Average $I/\sigma(I)$	49.11	68.61	25.16	30.80	5.90	8.48
R_{int}	0.021	0.016	0.035	0.029	0.049	0.032
Refinement						
$R[F^2 > 2\sigma(F^2)]$, $wR(F^2)$, S	0.055, 0.156, 1.02	1.106, 0.262, 1.07	0.053, 0.159, 0.99	0.051, 0.160, 1.03	0.068, 0.143, 1.11	0.112, 0.233, 1.10
No. of reflections	13 682	4554	10 060	5029	9089	5062
No. of parameters	626	217	453	240	679	285
No. of restraints	6	0	0	12	0	64
H-atom treatment	Riding, distances refined	Riding, distances refined	Riding, distances refined	Riding, distances refined	Riding, distances refined	Riding, distances refined
$\Delta\rho_{max}$, $\Delta\rho_{min}$ (e Å^{-3})	0.46, −0.30	0.63, −0.69	0.54, −0.28	0.43, −0.23	0.32, −0.25	0.69, −0.70

fully refined on the corresponding reflections. Refinement data of (2*a*sub) and a comparison with (2*a*) can be found in Table 2.

The quality indicators for the resulting structure are, as expected, significantly worse than those of the actual structure, and the large average displacement of the atoms in the actual structure from those in the averaged structure is reflected by the large and asymmetric anisotropic displacement parameters (Wagner & Schönleber, 2009; see Fig. 5). A CIF for the structure (2*a*sub) is included in the supplementary material.[1]

Prior to discussion of the factors that regulate this commensurate modulation of the three molecules in (2*a*), we will look at the first polymorph of the *iso*-propyl substituted Tröger's base analogue α-(3*a*), where we find not three, but two molecules in the asymmetric unit, with angles between the benzene ring planes of 95.58 (6) and 95.45 (6)°, and again the space group $P\bar{1}$, with D_x (100 K) = 1.194 g cm^{-3} and m.p. 382–383.5 K (Didier *et al.*, 2008). Even though the particulars are different, a layer structure is adopted which is very similar to that of the ethyl-substituted Tröger's base analogue (2*a*), even though there now is in fact inversion symmetry present between adjacent layers and pairs, but not within the pairs of molecules within the layer, and the commensurate modulation is thus reduced to a period of two molecules instead of three. This is depicted by the color coding in Fig. 6.

The pseudo-translation symmetry between two molecules ($x, y-\frac{1}{2}, z+\frac{1}{2}$, average r.m.s. distance for non-H atoms 0.34 Å) is again demonstrated by a refinement in a subcell [α-(3*a*sub)], which, with a disordered model for the affected *iso*-

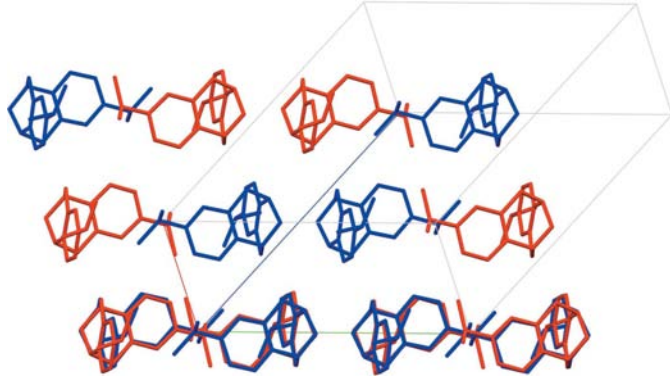

Figure 6
The packing of α-(3*a*), as viewed within the plane of the layers, in the direction of the pseudo-translation. Symmetry-equivalent molecules are coloured identically. The lower row of superimposed molecules clearly shows very good fit between pseudosymmetric molecules, except for the *iso*-propyl groups within the pairs of molecules.

[1] Supplementary data for this paper are available from the IUCr electronic archives (Reference: RY5032). Services for accessing these data are described at the back of the journal.

propyl group, essentially yields the same quality indicators as the parent model α-(3*a*): the disordered model describes the structure mathematically equally well as the commensurate modulation, with only half the number of reflections, *i.e.* under omission of the weaker and less accurately measured supercell reflections, making the overall *R* factor in this case even slightly better than for the commensurately modulated $Z' = 2$ structure. Apart from the presence of supercell reflections in the diffraction pattern of the $Z' = 1$ structure (which necessitate the consideration of the supercell with $Z' = 2$), the α-(3*a*sub) structure also displays methyl···methyl contacts between the disordered *iso*-propyl groups that are impossibly short [H···H 1.69 Å, average H···H distance in organic crystals 2.18 Å (Rowland & Taylor, 1996)]. For a CIF and displacement ellipsoid plot of α-(3*a*sub), see the supplementary material. For a comparison of crystallographic and refinement data between the structures of (2*a*) and α-(3*a*) and their respective substructures, see Table 2. The substructures (2*a*sub) and α-(3*a*sub) with $Z' = 1$ have the same packing motif and similar unit-cell dimensions, and are in all other respects isomorphous. For a graphical comparison between the structures of (2*a*), (2*a*sub), α-(3*a*) and α-(3*a*sub), see Fig. 7.

Of the 37 structures of symmetrically substituted Tröger's base [excluding compounds with benzene rings constituting part of larger (hetero)aromatic systems, salts, solvates, co-crystals and derivatives with substituents elsewhere than on the benzene rings] in the CSD, seven have the space group $P\bar{1}$, and all five with $Z' = 1$ pack very similarly to the structures (2*a*sub) and α-(3*a*sub). Commensurate modulation is absent in all five cases [CSD codes DICHIG (Larson & Wilcox, 1986), JEVYUF (Faroughi, Scudder *et al.*, 2007), NIFFEO (Faroughi *et al.*, 2007*a*), LAPCAH (Sergeyev *et al.*, 2005), XENGIH (Faroughi *et al.*, 2006)]. The other two structures (EDEWAM, 4,10-dibromo, 2,8-dimethyl; Faroughi *et al.*, 2007*b*; SOBGEW, 1,4,7,10-tetrabromo; Didier *et al.*, 2008) have $Z' = 2$, and pack differently, in columns instead of pairs.

The discussion of the packing motif of α-(3*a*) is somewhat more straightforward than for (2*a*): it can clearly be seen in the structure of α-(3*a*sub) that two methyl groups of the *iso*-propyl substituents contained within the cavity formed by the two Tröger's base skeletons are competing for the same space in the crystal. This leads to one *iso*-propyl group consistently adopting a different conformation, in that way destroying the inversion symmetry and doubling the unit cell.

Since the remainder of the Tröger's base skeleton is very close to being crystallographically dependent the two independent molecules in the asymmetric unit of α-(3*a*) have very similar CH···π interactions on both ends of the pair. A list of all contacts in α-(3*a*) shorter than the van der Waals radius can be found in Table S1 of the supplementary material. None of the atom–atom contacts listed in the table are stabilizing, as indicated by a UNI force-field calculation – all interaction energies between atoms below the van der Waals radius are slightly positive. The largest stabilization energies in the structure are found within molecular pairs, and between adjacent molecular pairs, and are easily attributed to CH···π and π···π interactions.

For (2*a*) the deviations from crystallographic symmetry are much larger, and not limited to just the ethyl group. This leads to larger differences in the intermolecular contacts between the three crystallographically independent molecules, and in these the reasons for adopting the modulation in the structure can be recognized. All contacts in (2*a*) shorter than the sum of the van der Waals radii are listed in Table S2. Again, none of the atom–atom contacts are attractive, and the main stabilization of the structure is due to CH···π and π···π interactions.

If we look at the sideways arrangement of the layers '1' and '2' (Fig. 3), it is clear that the respective benzene rings of Tröger's base in layer '2' (red molecules) overlap with voids left in layer '1' (yellow molecules) by the ethyl groups, which are both oriented perpendicular to the ring plane. This results in enough space for the benzene rings, and in ethyl groups which are sandwiched between two benzene rings of the layers '2', and forming stabilizing CH_3···π contacts within their pairs.

The situation is different between the two successive layers '2' – here the benzene rings (blue molecules in Fig. 3) and the voids in layer '1' do not overlap, and the

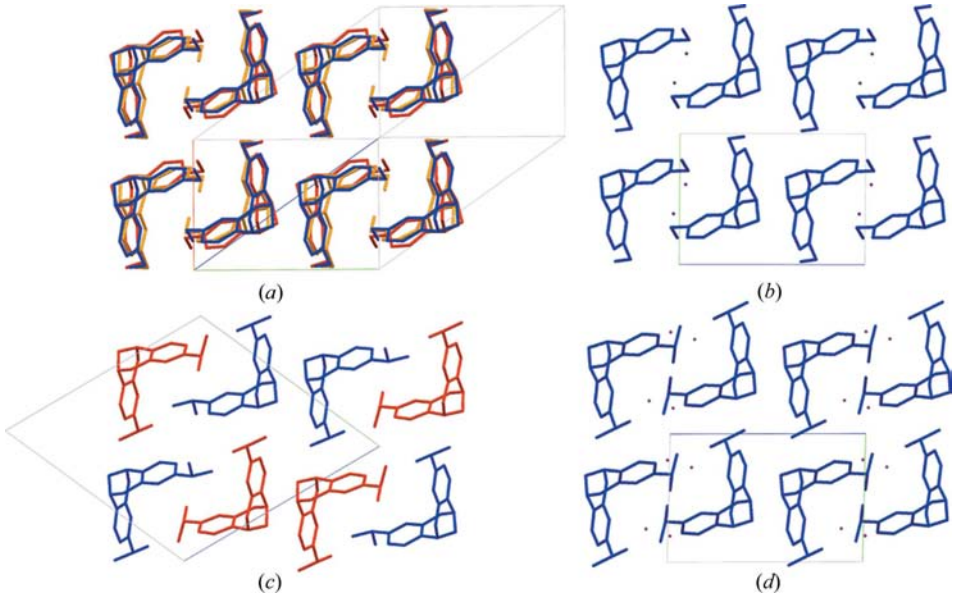

Figure 7
Comparison between the structures of (*a*) (2*a*), along [$\bar{1}\bar{1}1$]), (*b*) (2*a*sub) (along *a*), (*c*) α-(3*a*) (along **a**) and (*d*) α-(3*a*sub) (along *a*). Molecules are coloured according to their symmetry equivalence. Disordered atoms represented by unconnected dots.

two benzene rings now compete for the same space in the crystal. The red molecules do not suffer this same influence of their neighbours, and hence, for the sake of conservation of van der Waals contact stabilization, and avoidance of steric hindrance, the inversion symmetry within the red–blue pair is destroyed, and the $CH_3\cdots\pi$ contacts that aid in keeping the red–blue pairs together are deformed. As a result, the ethyl groups inside this cavity twist away from their perpendicular configuration in order to keep a suitable geometry for their $CH_3\cdots\pi$ contacts with the benzene ring of the other molecule in the pair. One of the ethyl groups (red) has to twist about 27° from perpendicular in order to keep a good contact geometry, but the other ethyl group (blue) has to twist to an almost entirely coplanar configuration with the benzene ring it is substituted on, and as a result starts interfering with a CH_2 group in layer '1' (H6*A*). This appears to be the origin of the observed disorder of the terminal methyl group – the balance between a better geometry for the $CH_3\cdots\pi$ contact but interference with the methylene group, or less interference, but loss of the stabilizing $CH_3\cdots\pi$ contact. The observed Fourier map (Fig. S2) shows two well defined peaks, corresponding to two equilibrium positions, and not a single smear that would correspond to a randomly moving methyl group in a featureless broad potential well.

We can conclude this section by stating that $CH\cdots\pi$ interactions appear to be the major stabilizing force in these crystal structures. This is corroborated by force-field calculations, which consistently show that the most stabilizing interactions are either those between molecules paired up centrosymmetrically or pseudo-centrosymmetrically, or those between adjacent pairs. In the case of stacks, the most stabilizing interactions are between successive molecules in a stack. All of these interactions display geometries that correspond to $CH\cdots\pi$ contacts, either between the alkyl substituents and the Tröger's base rings in a pair, or between the bridging methylene group and the Tröger's base rings between pairs or in stacks. All stabilization energies obtained by intermolecular attraction are small, with a maximum of 66 kJ mol^{-1} between two individual stacked molecules of (4*a*). A comparison between the lattice energies of the substructures and the structures with $Z' = 3$ and $Z' = 2$ reveals very small energy differences per molecule, that are likely to be within the error margin of the calculation (see Table S7). In addition, the disorder present in the molecules makes it almost impossible to draw firm conclusions with regard to the energy differences. Nevertheless, the energy differences that are calculated in this way do conform to our expectations – the structures with larger Z' are indeed slightly more stable. The modulation in the structures thus appears to be caused by a mismatch between the volumes of the substituents and that of the Tröger's base skeleton. It is only natural that the consequences are worse for the ethyl substituted molecule than for the *iso*-propyl variant, as the mismatch there is larger (which also leads to a substantially lower melting point and a lower calculated lattice energy per molecule). In the *iso*-propyl structure α-(3*a*) the substituents interfere with each other, leading to an alternating configuration between neighbouring molecules. The calculated lattice energies of the two disordered variants of the non-alternating substructure clearly demonstrate these *iso*-propyl–*iso*-propyl contacts in α-(3*a*) are strongly repulsive. The adoption of structures with $Z' > 1$ in these cases happens exclusively due to close packing and steric hindrance, and no strong or competing interactions are in any way involved. If a $Z' = 1$ structure would be adopted in these cases, this would either lead to voids in the structure or severe steric conflicts.

Crystals for enantiomerically pure (3) or (2) could not be obtained so far. One might be tempted to attribute this to the mismatch between substituent and skeleton size, combined with the additional complexity of the necessary complete absence of a centre of symmetry in enantiomerically pure Tröger's base structures, but of course no hard evidence can be obtained for this assumption.

In an attempt to verify whether or not α-(3*a*) would transform to a high-temperature phase with $Z' = 1$, we tried to obtain new single crystals, as the crystals on which the original experiment was performed were no longer available. The crystals which were now obtained by slow evaporation of CH_2Cl_2, however, showed a different habit, and a different unit cell, and turned out to be a different polymorph of (3), with a packing very similar to that of (4*a*). Full datasets were measured of this polymorph after flash-cooling to 100 K [β-(3*a*)]. Crystals of α-(3*a*) could not be regrown so far.

This second polymorph of *iso*-propyl Tröger's base, β-(3*a*) [D_x (100 K) = 1.181 g cm^{-3}, m.p. 383.5–384.5 K] is again a modulated structure at 100 K, with $Z' = 3$. The melting point is 1.5 K higher than for α-(3*a*), indicating this polymorph to be slightly more stable, which is corroborated by the force-field calculations (Table S7). Angles between the benzene rings in the three crystallographically independent molecules are 79.85 (9), 77.54 (9) and 76.96 (9)°. Despite the high Z', the structure is reminiscent of the structure of Tröger's base itself

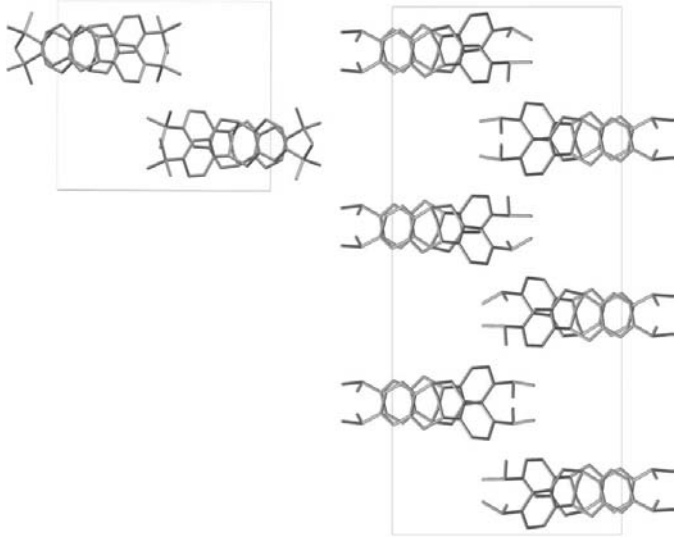

Figure 8
The columnar arrangement of β-(3*a*) (right) and (4*a*) (left) as seen down the column axis, which coincides with *c*.

(DILLEP), with stacks of alternating enantiomers, related by glide planes. The relative arrangement of the columns is different, resulting in the space group $P2_1/c$ as opposed to *Pccn* for native Tröger's base. This allows the *iso*-propyl groups to collect in alkyl-rich parts of the structure, while the basic packing between the Tröger's base skeletons is conserved (see Fig. 8).

The modulation is due to the *iso*-propyl group on one end of the molecule, with the group in one molecule having a different orientation than those in the other two. As in (2*a*), the repercussions for the rest of the structure are serious, and the entire Tröger's base skeleton is moved around substantially. The r.m.s. displacement of equivalent non-H atoms within the three molecules after pseudo-translation is on average 0.43, 0.54 and 0.24 Å between the different molecular pairs. This is illustrated in Fig. 9, showing the relative shifts of the molecules in the pseudo-translation direction.

Dividing the *b* axis by three yields a subcell, *β*-(3*a*sub), in which the structure can be refined on the integral reflections, but with considerable disorder, which has been modeled for the *iso*-propyl group, and which, predictably, yields occupancies very near 0.33 for the three different *iso*-propyl groups. The particulars of this refinement can be found in Table 2 (*β*-3*a*sub), and the CIF is part of the supplementary material. Short contacts for *β*-(3*a*) are listed in Table S3, and the structure again appears to be determined more by the overall shape of the van der Waals envelope of the molecules than by specific interactions, as confirmed by UNI force-field calculations.

The packing here is harder to rationalize than in (2*a*), due to the occurrence of more symmetry elements. In general, the organization of (2*a*), namely two kinds of layers, consisting now of columns instead of pairs, is adopted, as shown in Fig. 10.

The molecules with the *iso*-propyl group 'wrongly' oriented are the yellow ones in Fig. 10. This orientation is only possible due to the blue molecules having their *iso*-propyl group pointing the other way, which in turn makes it possible for the columns consisting of yellow and red molecules to become narrower, due to steric interference being removed from between their own *i*-propyl groups, making the overall packing more dense. Comparing the overlap of the lower red–yellow and blue–blue pairs in the lower row of Fig. 10, this can be clearly seen.

Variable-temperature measurements indicated a phase change around 130 K, and thus a second data set was then collected at 148 K *γ*-(3*a*). At this temperature the structure indeed had transformed to a high-temperature modification with $Z' = 1$. *γ*-(3*a*) can be refined with *β*-(3*a*sub) as a starting model. The results of the refinement indicate that the distance between the similarly oriented *iso*-propyl groups *A* and *C* becomes small enough to describe them with one set of coordinates. This simplification allows to also model the disorder of the benzene ring. A list of short intermolecular distances can be found in Table S4. The worst steric conflicts naturally take place between the different parts of the disordered *iso*-propyl group, clearly indicating that despite the disorder now probably being dynamic, the group is still all but free to move. As can be seen from the contact distances in Table S4, especially the minor conformer [42.9 (3)%] C16*B* and its own symmetry equivalent at $1-x, 1-y, -z$ are unlikely to occur at the same time in adjacent cells, pointing to a dynamic phenomenon. According to the UNI force-field calculations, this interaction is also the major contributor to the destabilization of the structure, by 199.1 kJ mol^{-1} between that molecular pair.

A third data collection at room temperature (293 K) showed no further significant changes and only a minimal

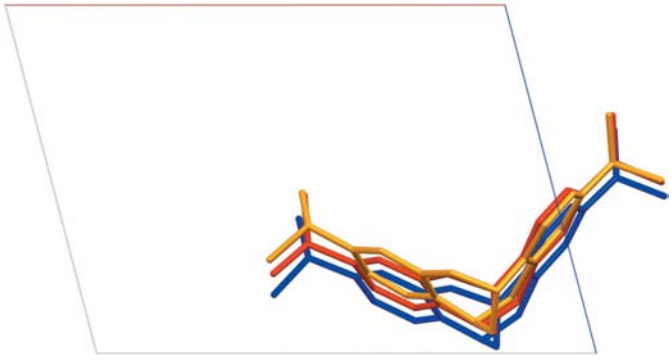

Figure 9
Superimposed view of the three symmetry-independent molecules in the structure of *β*-(3*a*) displaying pseudo-translation symmetry in the [010] direction.

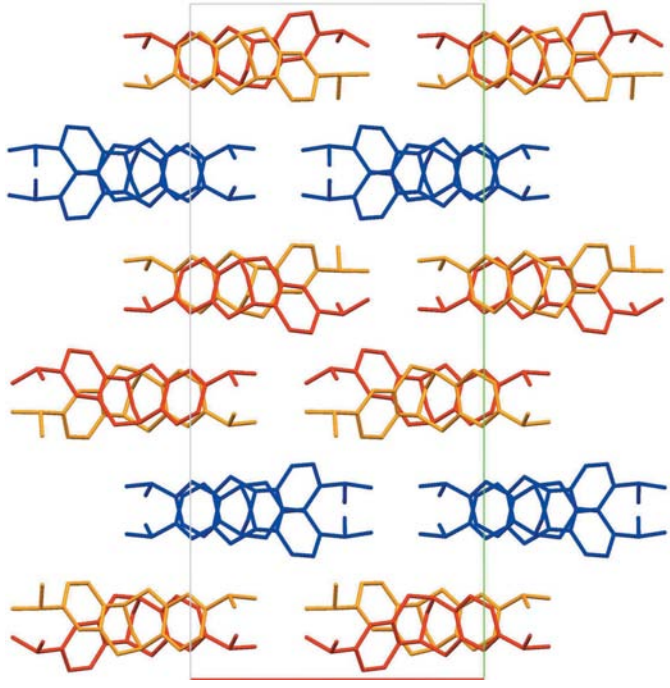

Figure 10
The packing of *β*-(3*a*) viewed down the *c* axis, with symmetry-equivalent molecules coloured identically. For further explanation, see text.

increase in the population of the 'wrong' *iso*-propyl group [46.3 (8)%]. The thermal movement of atoms, especially of the disordered *iso*-propyl groups, makes interpretation of the disorder difficult at this temperature.

Finally, the crystal was warmed up and cooled down slowly (< 1 K min^{-1}) while collecting individual frames of data at each temperature. This demonstrated that the phase change is both sharp and reversible in both directions, and occurs between 130 and 131 K (see Fig. S3). It would be logical to assume that the situation is comparable for (2*a*), and perhaps for α-(3*a*), but we have no experimental confirmation for this assumption. For α-(3*a*) the average structure α-(3*a*sub), like γ-(3*a*), appears to display contacts that are too close to be feasible, even with additional thermal motion at room temperature. What could be feasible for α-(3*a*) is a high-temperature structure where the alternation of differently oriented *iso*-propyl groups within successive pairs of molecules is conserved, but is no longer synchronized between different layers, which would lead to the disappearance of the supercell reflections. Due to the 'disappearing polymorph' problem, we are currently unable to provide an experimental verification.

Racemic *tert*-butyl Tröger's base analogue (4*a*) [D_x (90 K) = 1.162 g cm^{-3}, m.p. 480–482 K; Didier *et al.*, 2008] has an angle between the benzene ring planes of 102.29 (9)°, and is in all other respects isostructural to γ-(3*a*), but is itself not modulated (see Fig. 8).

Short contacts are listed in Table S5, and the structure again appears to be determined more by shape than by specific interactions.

Enantiopure *tert*-butyl Tröger's base analogue (4*b*) [D_x (100 K) = 1.127 g cm^{-3}] crystallizes in the space group *C*2, with two independent molecules in the asymmetric unit. The melting point of (4*b*) is 449–450 K, in accordance with Wallach's rule (see Brock *et al.*, 1991, and references cited therein). The angles between the benzene ring planes within the molecules are 103.5 (1) and 102.5 (1)°. It adopts a packing according to the 'pairwise strategy', with the end groups filling the cavity between the two molecules (Fig. 11).

Here of course, the two molecules in the pair cannot be symmetrically related by an inversion centre as they are the same enantiomer. The symmetry relationship between the two would have to be a (non-crystallographic) twofold rotation axis, if not for one of the external *tert*-butyl groups, which is rotated with respect to the other molecule. Even though this situation is somewhat similar to that of the *iso*-propyl groups in α-(3*a*), (4*b*) cannot be described as a commensurately modulated structure – in order to have pseudo-translation symmetry (*i.e.* layers in the *ac* plane), the pseudo-twofold axis within the molecular pair would have to be parallel with the crystallographic twofold axis, in which case the structure could be described in *P*2. Here, the deviation is about 15°. Thus, in contrast with the structures of (2*a*) and α-(3*a*), there are no layers here in the *ac* plane. Compound (4*b*) has adapted itself to the necessary absence of a centre of symmetry by forming a bi-molecular entity which is brick-shaped and easier to stack according to the twofold symmetry that is allowed, and in this way succeeds in mitigating the awkward shape of the molecule, again at the cost of raising Z' to 2.

This packing creates two small voids of 39 Å^3. The residual density in the voids (0.31 e Å^{-3}) was not modeled further. The presence of voids would explain the anomalously low density of the compound. All short contacts are listed in Table S6. The slight disorder in one of the *tert*-butyl groups, apparent from the shape of the displacement ellipsoids, was not further modelled, as it is very likely dynamic, and modelling it would do little but add to the confusion about atomic numbering.

4. Conclusion

In conclusion, we have provided structures of the Tröger's base skeleton with various conformationally flexible alkyl substituents. Systematically bringing a number of Tröger's base derivative structures together in this way has made it clear that there are two practical approaches for Tröger's base derivatives to crystallize, namely either in pairs or in stacks. Whether the compounds are racemic or enantiopure apparently plays no part in this choice, and the preference of a particular molecule for one or the other arrangement does not have a single determining factor, but is the result from the subtle differences in van der Waals interactions between the molecule and its environment. Owing to the conformational flexibility of both the skeleton itself and the substituents, the mismatch between the volume of the skeleton and of the substituents, and the flexibility of the weak stabilizing contacts in these crystals (typically CH$\cdots\pi$ or $\pi\cdots\pi$ interactions, which have a shallow potential well and a weak angular dependence; see *e.g.* Desiraju & Steiner, 1999, and references cited therein), we infer that the structures are able to obtain closer packing, better space filling and thus better van der Waals contact stabilization by expanding the size of their asymmetric unit,

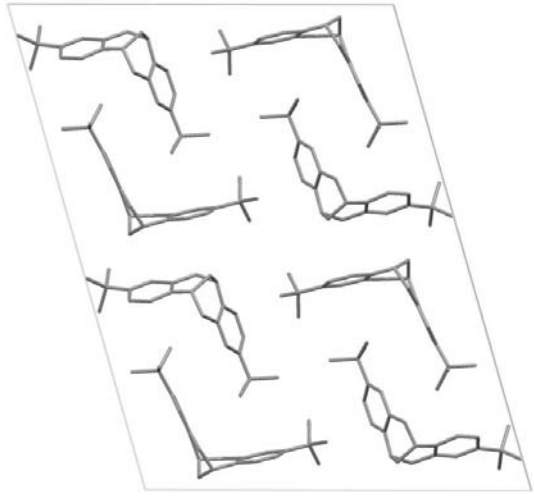

Figure 11
Packing of (4*b*), viewed down the *b* axis. The column consisting of four molecules on the right side is slanted down into the page towards the top of the picture, while the column on the left is slanted down towards the bottom of the picture.

without an appreciable energetic penalty in their other interactions. A small energetic benefit is evident from UNI force-field calculated sublimation enthalpies (see Table S7). This appears to corroborate a variant of the view of Hao *et al.* (2005), as already mentioned in the introduction – high Z' structures are often [but not necessarily, see *e.g.* (4*b*)] a modulation of a parent structure, the important point being that a minimization of the mismatch of spacing between the molecules occurs. $Z' > 1$ in this case leads to structures that are more stable than their $Z' = 1$ counterparts, whether they are modulated or not. If the energy difference between the $Z' = 1$ structure and the modulated structure observed is offset by a larger $\mathrm{d}(\Delta S)/\mathrm{d}T$ of the $Z' = 1$ structure, the $T\Delta S$ term in the free-energy expression can give rise to a phase transition when the temperature increases, as clearly evidenced in γ-(3*a*).

In all cases here structures result with one, two or three whole molecules in the asymmetric unit (and in one case also some additional disorder), whereas the minimal size of the asymmetric unit for these compounds is always half a molecule, related to the other half by a twofold rotation axis. For crystal structures of organic compounds, a twofold rotation axis as a molecular symmetry element is on average conserved as crystal symmetry in 60% of the cases (Pidcock *et al.*, 2003), whereas in the aforementioned 37 published structures of Tröger's base analogues, conservation of the molecular C_2 symmetry occurs in only nine cases (24.3%), of which one has $Z' = 1.5$, and another crystallizes in $P2/c$ with two crystallographically independent half molecules (CSD refcode YUPMOM; Faroughi *et al.*, 2009). This pointedly illustrates the compromise between close packing and long-range order that has to be reached by flexible structures with weak stabilizing interactions, and establishes substituted Tröger's bases firmly in the section of 'awkwardly shaped' molecules that are difficult to tessellate. No strong directional interactions are evident in the structures. These crystals were not grown under kinetic conditions (slow solvent evaporation over days or weeks at room temperature), and can thus reasonably be assumed not to be a trapped high-energy form. Evidence exists that for the β-(3*a*)–γ-(3*a*) pair the transition between high Z' and low Z' modifications is thermodynamic. Finally, it can thus be expected from this small set of structures that Tröger's base's peculiar, chiral, bicyclic, 'v'-shaped molecular skeleton will, in the absence of strongly stabilizing, directional crystal synthons, yield many more high-Z' structures, based on no other molecular properties than its awkward shape and its chirality.

The authors thank Delphine Didier and Adrienne Remacle for the help with the enantioseparation of (2)–(4), Mateusz Pitak for technical assistance with XRD data collection, and Yves Geerts for providing laboratory resources and allowing SS the opportunity to conduct an independent research program in his laboratory at ULB. BT is a fellow of the F.R.I.A. This study was in part supported by the F.N.R.S., and the Smart Apex diffractometer was funded by NSF grant 0087210, by Ohio Board of Regents grant CAP-491, and by YSU. The authors wish to thank the co-editor and an anonymous reviewer for comments that have substantially improved the manuscript.

References

Allen, F. H. (2002). *Acta Cryst.* B**58**, 380–388.
Anderson, K. M., Goeta, A. E. & Steed, J. W. (2008). *Cryst. Growth Des.* **8**, 2517–2524.
Anderson, K. M. & Steed, J. W. (2007). *CrystEngComm*, **9**, 328–330.
Brock, C. P., Schweizer, W. B. & Dunitz, J. D. (1991). *J. Am. Chem. Soc.* **113**, 9811–9820.
Bruker (2008). *SAINT*, Version 7.XX. Bruker AXS Inc., Madison, Wisconsin, USA.
Bruno, I. J., Cole, J. C., Edgington, P. R., Kessler, M., Macrae, C. F., McCabe, P., Pearson, J. & Taylor, R. (2002). *Acta Cryst.* B**58**, 389–397.
Desiraju, G. R. (2007). *CrystEngComm*, **9**, 91–92.
Desiraju, G. R. & Steiner, T. (1999). *The Weak Hydrogen Bond.* Oxford: Oxford Science Publications.
Didier, D., Tylleman, B., Lambert, N., Vande Velde, C. M. L., Blockhuys, F., Collas, A. & Sergeyev, S. (2008). *Tetrahedron*, **64**, 6252–6262.
Dolenský, B., Elguero, J., Král, V., Pardo, C. & Valík, M. (2007). *Adv. Heterocycl. Chem.* **93**, 1–56.
Faroughi, M., Jensen, P. & Try, A. C. (2009). *ARKIVOC*, **10-ii**, 269–280.
Faroughi, M., Scudder, M., Turner, P., Jensen, P. & Try, A. C. (2007). *Acta Cryst.* E**63**, o1048–o1050.
Faroughi, M., Try, A. C. & Turner, P. (2006). *Acta Cryst.* E**62**, o3674–o3675.
Faroughi, M., Try, A. C. & Turner, P. (2007*a*). *Acta Cryst.* E**63**, o2695.
Faroughi, M., Try, A. C. & Turner, P. (2007*b*). *Acta Cryst.* E**63**, o3030.
Farrugia, L. J. (1997). *J. Appl. Cryst.* **30**, 565.
Farrugia, L. J. (1999). *J. Appl. Cryst.* **32**, 837–838.
Filippini, G. & Gavezzotti, A. (1993). *Acta Cryst.* B**49**, 868–880.
Gavezzotti, A. (2003). *OPiX*. University of Milano, Italy.
Gavezzotti, A. (2008). *CrystEngComm*, **10**, 389–398.
Gavezzotti, A. & Filippini, G. (1994). *J. Phys. Chem.* **98**, 4831–4837.
Hao, X., Chen, J., Cammers, A., Parkin, S. & Brock, C. P. (2005). *Acta Cryst.* B**61**, 218–226.
Larson, S. B. & Wilcox, C. S. (1986). *Acta Cryst.* C**42**, 224–227.
Pidcock, E. (2006). *Acta Cryst.* B**62**, 268–279.
Pidcock, E., Motherwell, W. D. S. & Cole, J. C. (2003). *Acta Cryst.* B**59**, 634–640.
Prelog, V. & Wieland, P. (1944). *Helv. Chim. Acta*, **27**, 1127–1134.
Rowland, R. S. & Taylor, R. (1996). *J. Phys. Chem.*, **100**, 7384–7391.
Sergeyev, S. (2009). *Helv. Chim. Acta*, **92**, 415–444.
Sergeyev, S., Schär, M., Seiler, P., Lukoyanova, O., Echegoyen, L. & Diederich, F. (2005). *Chem. Eur. J.* **11**, 2284–2294.
Sheldrick, G. M. (2008). *Acta Cryst.* A**64**, 112–122.
Spek, A. L. (2009). *Acta Cryst.* D**65**, 148–155.
Steed, J. W. (2003). *CrystEngComm*, **5**, 169–179.
Tröger, J. (1887). *J. Prakt. Chem.* **36**, 225–245.
Wagner, T. & Schönleber, A. (2009). *Acta Cryst.* B**65**, 249–268.
Worlitschek, J., Bosco, M., Huber, M., Gramlich, V. & Mazzotti, M. (2004). *Helv. Chim. Acta*, **87**, 279–291.